

## Chapter 10

# Microoptical Artificial Compound Eyes

Andreas Brückner, Jacques Duparré, Frank Wippermann, Peter Dannberg,  
and Andreas Bräuer

**Abstract** The cost–benefit ratio of miniaturized single aperture eyes underlies certain limitations, so that evolution led to the development of multi-aperture eyes in case of tiny creatures like invertebrates. Physical constraints, which also apply for the miniaturized artificial imaging systems, make this natural evolutionary path comprehensible. Shrinking down to a sub-millimeter range, the use of parallel imaging with multi-aperture systems is crucial. In this domain, microoptical design approaches and fabrication techniques are the solution of choice. This technology allows the realization of cost-efficient miniaturized imaging systems with sub-micron precision by means of photolithography and replication. The approaches proposed here are mainly inspired by insect vision in nature, although they are bound to planar substrates.

### 10.1 Introduction

Vision is by far the most important sense for 3D navigation or guidance of autonomous flying vehicles. However, vision is also a costly sense for miniaturized systems due to the demands of size, weight, power consumption, and speed for the necessary sensor components on board. Even the simplest vision system requires optics to form an image of the environment, an image sensor to convert image illumination into electric current, processors to interpret visual information for guidance, electronics, and a power supply.

When examining state-of-the-art miniaturized camera systems we learn that the lens is usually the bulkiest component with a minimum size of about 4 mm along each side. In the following section we are going to discuss where this limit originates from and why a simple miniaturization of classical optics would drastically reduce the image resolution. But how can this limitation of optics be overcome? A fascinating approach is to look how nature has successfully solved similar problems in the case of very small creatures like insects which solely use compound eyes.

During the last century, the optical performance of natural compound eyes was analyzed exhaustively [39]. Following the terminology found in literature, we will distinguish between two major classes of compound eyes: (1) the apposition compound eyes and (2) the superposition compound eyes [31]. Within the scope of this chapter we are going to give a coarse overview of the different optical working principles, what their advantages and drawbacks are, and how they inspired the development of artificial compound eye optics.

Several technical concepts and realizations of imaging sensors using multiple optical channels<sup>1</sup> have been presented in the last two decades. However, since the major challenge for a technical adoption of natural compound eyes is the required fabrication and assembly accuracy, none of these attempts has led to a breakthrough, since classical macroscopic fabrication technologies were exploited to manufacture microscopic structures. A more appropriate way to build up the required microstructures with high precision in

---

A. Brückner (✉)  
Fraunhofer Institute for Applied Optics and Precision  
Engineering, Albert-Einstein-Str. 7, D-07745 Jena, Germany  
e-mail: andreas.brueckner@iof.fraunhofer.de

---

<sup>1</sup> In the following the term multi-channel imaging systems will be used.

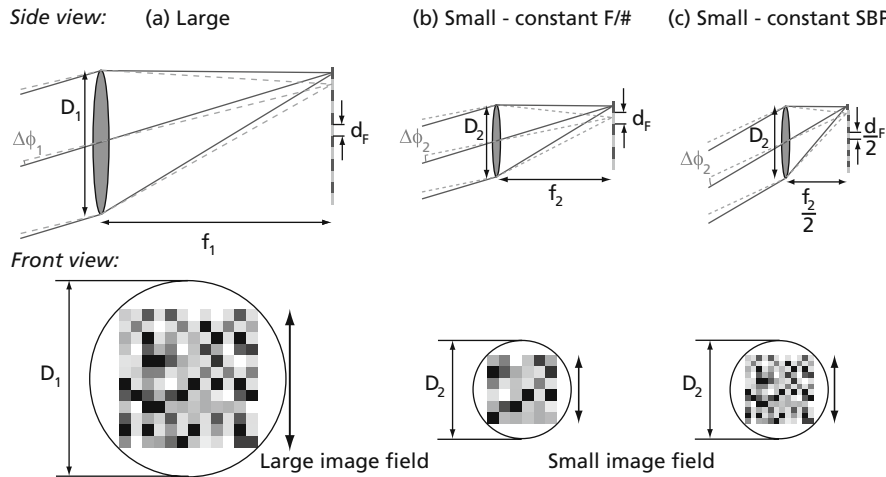


**Fig. 10.1** Scaling of lenses with constant  $F/\#$  (b) or space-bandwidth-product (SBP) (c). (a) *Large lens*: The size of one image point is proportional to  $\lambda F/\#$ . Due to the large focal length  $f_1$  the angular projection of an image point into object space  $\Delta\phi_1$  is very small. The lens has a high angular resolution and a large information capacity caused by the extension of the image field and the small spot size. (b) *Small lens with same  $F/\#$* : The size of one image point is the same as in (a). However, due to the short focal length  $f_2$ , here the angular projection of one spot

$\Delta\phi_2$  is enlarged. Hence the lens has a low angular resolution and reduced information capacity due to the small image field size. (c) *Small lens with same information capacity*: The spot size is decreased due to the reduction of the  $F/\#$ . The same angular resolution as in (b) results as the focal length is decreased with the size of one image point. Consequently, the information capacity in the image plane equals that of the large system but the information is gathered from a larger field of view with reduced angular resolution. Adopted from [46]

a cost-efficient manner is to rely on state-of-the-art microoptics technology being adapted from semiconductor fabrication techniques.

In this chapter, we present a way to design and fabricate microoptical artificial compound eyes. Although these systems are inspired by the insect eye, they are not intended to be a copy of it. We rather adopted some design rules to achieve ultra-compact optical sensors with the major advantages like the small overall size and low weight in combination with a large field of view. These are demands of applications in the fields of machine vision, security, surveillance, and medical imaging. However, they will also be a benefit to the visual guidance system of flying micro-robots or portable consumer electronics. Compound eye sensors can, for instance, fit into tight spaces like credit cards, stickers, sheets, or displays.

## 10.2 Miniaturization of Imaging Systems

For understanding the existence of compound eyes which is at least partly caused by physical limitations of the miniaturization of optical systems, we will have to glimpse at some well-known principles of optics. As a reward, the following little optical excursion will shed some light on the promises but also on the limits of artificial compound eyes.

From the point of view of an optical design engineer, shrinking the size of a classical optical system<sup>2</sup> is fine because geometrical imaging errors (often called aberrations) drastically decrease with the aperture size [41]. From this standpoint we might say that the smaller the size of a vision system, the easier the formation of a good (meaning sharp) image. However, from physical optics we know that light can never be focused to a perfect point image. Even when using an optically ideal constructed lens with a focal length  $f$  and an aperture diameter  $D$  the image of a (perfect) point-like object will have a finite size which is proportional to the ratio<sup>3</sup>  $F/\# = f/D$  and the wavelength  $\lambda$  of light. Due to this phenomenon of diffraction the size of the smallest image feature is the so-called diffraction limited spot size. As there is a certain smallest image feature size and a certain image field size, the number of image details that are captured by a vision system (or its information capacity) is also limited. For that reason, the stop number  $F/\#$  should either stay constant

<sup>2</sup> Due to its single channel setup including one or a few lenses and at least one aperture, all aligned on a common axis, we will further call this single aperture optical system.

<sup>3</sup> This ratio is called the stop number or F-number  $F/\#$ .

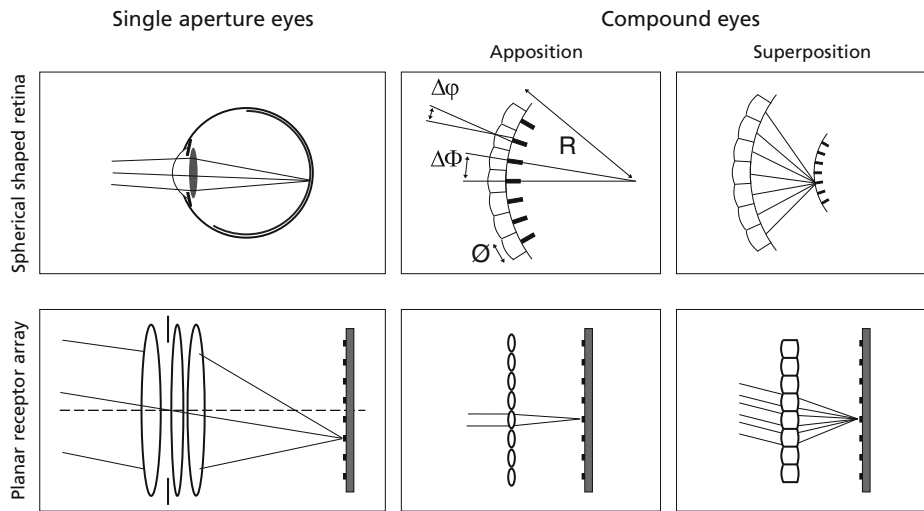


**Fig. 10.2** Different types of natural eye sensors (*top*) and their technical counterparts (*bottom*) [46]

or shrink in order to preserve image resolution (Fig. 10.1b) or information capacity (Fig. 10.1c) – referred to as space-bandwidth-product (SBP) – during miniaturization [33].

We may conclude that the miniaturization of a single aperture optical system has to be paid by a reduction of either the angular resolution or the information capacity. A certain minimum system size is needed for a high image and angular resolution. The evolutionary solution of choice is found in the vision systems of tiny creatures like invertebrates – the compound eye. Here, a large number of extremely small vision systems (called ommatidia) on a curved basis capture the visual information of a large field of view (FOV) in parallel. The use of parallel optical channels breaks the trade-off between focal length and the size of the FOV. Although each ommatidium exhibits a small FOV and thus a small information capacity, the sum of all ommatidia of the compound eye provides a large FOV (often nearly  $180^\circ$ ) and large information capacity so that accurate and fast flight maneuvers such as known for instance from flies are possible (details can be found in Chap. 4).

The multi-aperture solution is well adapted not only to the external skeleton but also to weight and metabolic energy consumption of small invertebrates. Due to the very short focal length of each microlens, compound eyes have a large depth of focus. Hence there is no need for a focusing mechanism. Compared to the mammalian single aperture eye, the amount of gathered optical information is low which suits the capacity of an insect's brain. However, the arrangement of the ommatidia on a spherical shell is a major advantage which allows a very large field of view while its total volume remains small. Hence, the main volume of the head is still available for the brain and signal processing. In nature, the lack of high angular resolution is often counterbalanced by high temporal sampling<sup>4</sup> and additional functionalities such as polarization sensitivity, hyperacuity, or fast movement detection [35,45].

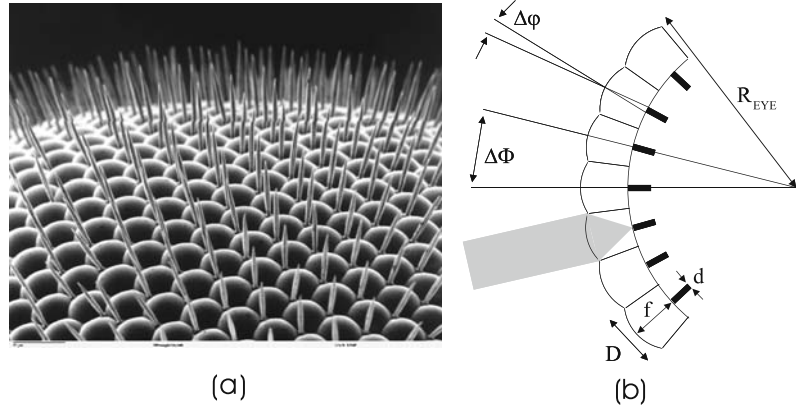
Natural compound eyes have been subject to scientific research for more than a century. As this section covers only some essential basics of natural compound eye vision, references [31] and [39] are especially recommended for further reading.

### 10.3 The Compound Eyes of Insects

The classification of compound eyes can be divided into apposition and superposition compound eyes (Fig. 10.2) [31,39,43].

<sup>4</sup> Compared to the temporal sampling of human vision of about 25 frames per second a fly samples about 10 times faster (approx. 250 Hz) [13].

**Fig. 10.3** Natural apposition compound eye. (a) Scanning electron microscope (SEM) image detail of the compound eye of a fruit fly (“*Drosophila*”). (b) Principle of a natural apposition compound eye which is composed of a large number of ommatidia arranged on a curved basis with radius  $R_{\text{EYE}}$ .



### 10.3.1 Apposition Compound Eyes

In natural apposition compound eyes, which mainly evolved in day-active insects such as flies (Fig. 10.3a), each microlens is associated with a single photoreceptor in its focal plane [11]. One could find several hundreds (water fly) up to tens of thousands (Japanese dragon fly) of these single microlens-receptor units which are commonly referred to as ommatidia. The intermediate space between adjacent ommatidia is filled with pigments that form opaque walls to prevent light from leaking out from one ommatidium into the next which would cause optical cross-talk [28].

The optical axis<sup>5</sup> of each ommatidium points to a different direction (Fig. 10.3b) so that nearly 360° of the visual surrounding is sampled in patches defined by the interommatidial angle

$$\Delta\Phi = D/R_{\text{EYE}}. \quad (10.1)$$

Hence, Eq. (10.1) gives the angular offset between the optical axes of two adjacent ommatidia with diameter of the microlens  $D$  and the radius of the eye  $R_{\text{EYE}}$ . The photoreceptor in each ommatidium accepts light from an angular interval  $\Delta\phi$ . In fact, the angular response is approximately a Gaussian centered on the corresponding optical axis [11,16]. The so-called acceptance angle  $\Delta\phi$  is its full width at half maximum. It is one of the most important parameters of a com-

pound eye because it determines the trade-off between sensitivity and resolution. The acceptance angle has a geometrical contribution  $\Delta\rho = d/f$  which is determined by the photoreceptor diameter  $d$  projected into the object space (via the focal length  $f$ ). A second contribution  $\lambda/D$  originates from the diffraction at the microlens aperture  $D$  for the wavelength  $\lambda$  [42], resulting in

$$\Delta\phi = \sqrt{\left(\frac{d}{f}\right)^2 + \left(\frac{\lambda}{D}\right)^2} \quad (10.2)$$

A large  $\Delta\phi$  means that each ommatidium collects light from a large angle, therefore the sensitivity is high but the resolution is low meaning that two object points which are separated by a small angle would be imaged on a single receptor. Vice versa, a small acceptance angle causes higher resolution but lower sensitivity. For that reason it is insufficient to just increase the number of ommatidia of a compound eye while keeping the acceptance angle constant in order to increase the total resolution. Instead, the ommatidia must increase in both number and size [1] which is the reason why there are no large compound eyes found in nature. When a certain size is exceeded for the compound eye a much lower resolution results as compared to a single aperture eye of same size [24]. Many invertebrates developed compound eyes which have areas with a locally higher resolution than elsewhere in the eye. These “acute zones” point into the direction of highest interest, similar to the fovea in the eyes of mammals [15,29].

A special form of apposition compound eye, which can be found in several flies, comprises a set of photoreceptors in each ommatidium in contrast to a single

<sup>5</sup> Optical axis denotes the straight line which connects the center of a single microlens with the center of the associated photoreceptor. Thus, “axially” means in direction along the optical axis.

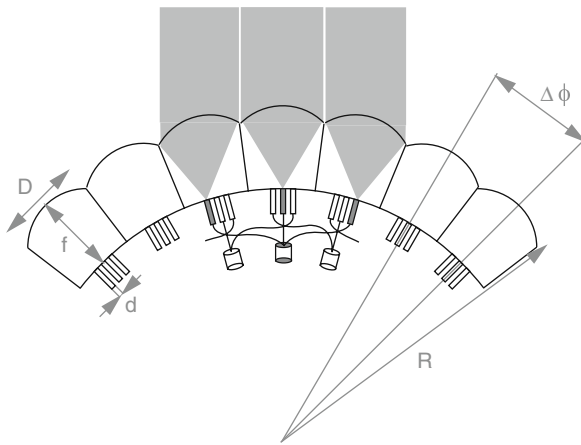


**Fig. 10.4** Working principle of a neural superposition eye. The optical axes of different photoreceptors from adjacent ommatidia point on the same location of a distant object

one. Here, each object point is imaged by multiple photoreceptors from different ommatidia and the related signals are fused in the first synaptic layers of the eye (see Fig. 10.4). Therefore, the setup is known as the neural superposition type of an apposition compound eye [13,25]. This multiple sampling of the same part of the field of view<sup>6</sup> enables an increased light sensitivity.

The main drawback of the apposition compound eye is a limited sensitivity which restricts their owners to live at daytime.<sup>7</sup> It might be for that reason that evolution came up with the second class of multi-aperture vision systems – the superposition compound eyes – for insects that are active at night.

### 10.3.2 Superposition Compound Eyes

The superposition compound eye (Fig. 10.5) has primarily evolved in night-active insects and deep water crustaceans due to the low-light conditions found in their habitats. In contrast to the apposition type, the focused light from multiple ommatidia combines on the surface of the photoreceptor layer to form a single

real image of the surrounding [31]. The decisive advantage of superposition compound eyes is that they are much more light sensitive because light bundles from one object point traveling through several adjacent ommatidia are deflected toward a common image point (Fig. 10.5b), increasing the light-collecting aperture  $D$  to a size which is several times larger than the diameter of the individual ommatidium. This optical performance is not the result of a single microlens per ommatidium but of two axially aligned microlenses that form a microtelescope [34]. In nature, eyes with small effective  $F/\#$  (ratio of eye's focal length  $F$  and diameter of the superposition aperture  $D$ ), even smaller than one, can be observed. However, blurring – caused by the imperfect combination of light beams from several ommatidia – lead to a resolution below the diffraction limit [30]. When comparing apposition with superposition eyes, it is evident that the clear zone that is needed for the fusion of light bundles leads to a larger volume in case of superposition compound eyes – a price that is paid for their higher sensitivity.

## 10.4 Insect-Inspired Imaging Systems

What can we learn and adapt from nature concerning the miniaturization of imaging systems? In multi-aperture eyes of insects the overall field of view is split into a number of fragments which are imaged by different optical channels in parallel. Each channel has a small information capacity but in total all channels achieve the capacity of a much larger optical system. Second, as each ommatidium images only a small angular segment around its optical axis, there are few geometrical imaging errors so that a very simple optical element, such as a single spherical lens, may be used.

After the first description of the potential of artificial compound eyes by Sanders and Halford [40], various technical approaches for compact vision systems exploited the basic principle of apposition compound eyes so far [9,12,17,26,36,49]. Latest developments in this field led to a novel 3D microfabrication method to develop artificial compound eye optics on a spherical basis [21,32]. However, the problem of recording the image from the curved image field of the eye still remains unsolved.

<sup>6</sup> In the following this will be called “redundant sampling.”

<sup>7</sup> Even though the neural superposition type could expand activities of its owner into light conditions of dawn and dusk.

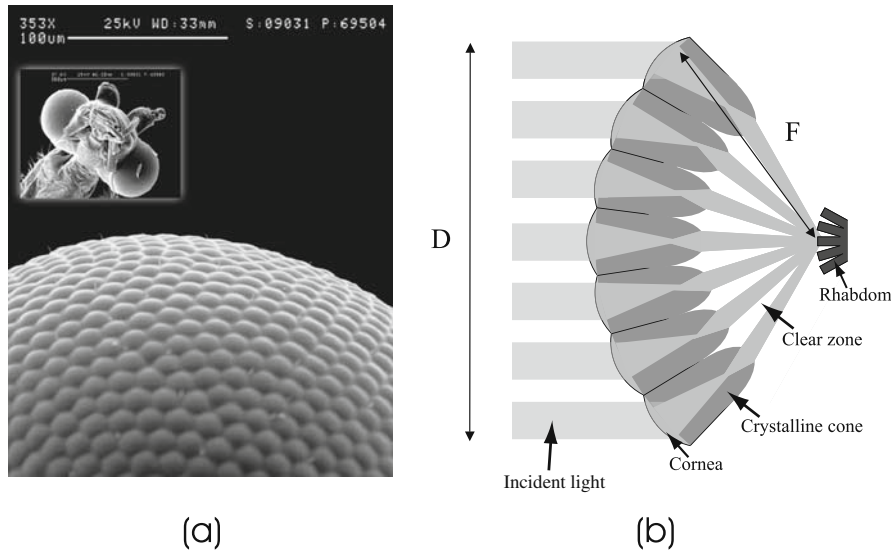


**Fig. 10.5** Natural superposition compound eye. (a) SEM image of head and eye section of the moth “*Ephestia kuehniella*.” (b) Schematic cross section of a natural superposition compound eye

In the case of the superposition compound eyes only a few technical equivalents have been demonstrated so far. Most remarkably, in 1940 Gabor published a setup of two stacked lens arrays with slightly different pitch axially separated by the sum of their focal lengths which would act like a normal (big) lens [10].<sup>8</sup> More than 50 years later, this planar derivative of superposition compound eye optics has been demonstrated experimentally [14]. But due to high technological and assembly efforts the setup has not yet found access to general applications. Systems with unity magnification using gradient-index lens arrays like found in photocopying machines and scanners are an exception [2,19,20,23].

Up to date, we have to conclude that only a few multi-aperture imaging systems found a successful way into application. The reason is that most of the published examples have been fabricated in macroscopic scale, so that assembly misalignments become critical when placing one channel beside each other, also lacking a considerable miniaturization. Microoptical fabrication technologies, instead, are promising for the fabrication of artificial compound eyes with a large number of channels. Fabrication and assembly tech-

nologies with high lateral precision may lead to cheap and compact imaging devices because a large number of systems can be manufactured in parallel processes.

#### 10.4.1 Artificial Apposition Compound Eyes

An artificial apposition compound eye in its simplest form consists of a planar 2D microlens array on a transparent substrate positioned on an optoelectronic detector array (Fig. 10.6) [5]. The thickness of the substrate is matched to the focal length of the individual microlenses  $f$  so that the detector pixels are located in the focal plane of the microlens array. As technical detector arrays such as CCD- or CMOS sensors are fabricated on planar substrates, a difference between the center-to-center spacing of the microlenses  $p_L$  and the pixels  $p_P$ <sup>9</sup> is used to achieve different viewing directions for the individual channels. Thus, the angular sampling scheme of the curved natural apposition compound eye is adapted to a planar setup. Each chan-

<sup>8</sup> Such a setup became known as the “Gabor superlens.”

<sup>9</sup> This is referred to as pitch difference  $\Delta p$ .



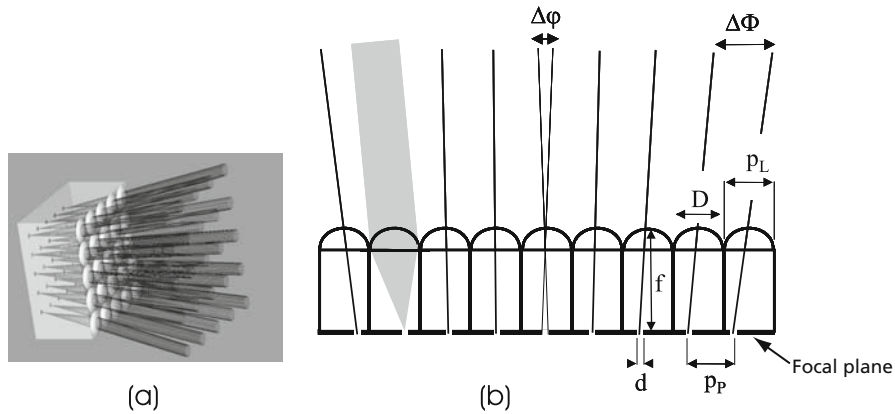


**Fig. 10.6** Schematic layout of a planar artificial apposition compound eye. (a) 3D model of the system showing the focusing microlens array, the pixel array in its focal plane, and the tilted optical axes of the specific channels sampling the field of view.

(b) Schematic section of the objective. The diameter of the individual microlens is  $D$  and  $d$  denotes the pixel size. See text for explanations

nel corresponds to one field angle in object space with the optical axis directed outward.

Another possibility of explanation is the so-called moiré magnifier [22,44]: Behind each microlens the (same) small image of the distant object is formed. Due to the result of the pitch difference between microlens and pixel array,  $\Delta p = p_L - p_P$ , the image is sampled at a slightly different location in each channel. When looking at the entirety of all sampled pixels a magnified version of the image is obtained from this sampling scheme. The overall image size of the artificial apposition compound eye is determined by the moiré magnification  $p_P / \Delta p$  and thus completely independent of the focal length. This arrangement delivers an image with a much larger magnification than that of a single microlens and at the same time it has a much shorter system length than a single aperture optical system with same magnification [5,6].

Analogous to the insect apposition compound eye we define the two most important system parameters: the angle between two adjacent optical axes (sampling angle), given by

$$\Delta\Phi = \arctan \frac{\Delta p}{f}, \quad (10.3)$$

and the acceptance angle  $\Delta\phi$  approximated by Eq. 10.2 where  $d$  is now the detector pixel diameter.

A further advantage of the artificial apposition compound eye is the large depth of field. As a result of the extremely short focal length of the microlenses an

object is focused independently of the object distance. This means that there is no need for an active focus adjustment.

#### 10.4.1.1 Prototype Demonstration

The conception and optical design of an artificial apposition compound eye start with selecting a suitable detector array. The pixel pitch of the detector array has to be in the range of 50–150  $\mu\text{m}$  while the photodiodes of each pixel should be small (between 2 and 10  $\mu\text{m}$ ), which is rather unusual for commercially available arrays. For that reason, standard detector arrays of large size can be used while only a fraction of the whole amount of pixels is read out. Alternatively, a customized image sensor array can be used, which additionally offers the possibility of implementing signal pre-processing within the vacant periphery of each pixel.

A recent prototype of an artificial apposition compound eye sensor that has been developed for passenger monitoring in automotive applications is shown in Fig. 10.7, its specifications are given in Table 10.1. Its main purpose is the detection of the seating position of a passenger in order to control the airbag inflation and prevent injuries caused by it in case of an accident. An artificial compound eye suits this application well as it demands a large field of view, a rigid system of low complexity with a large depth of field and fast pro-

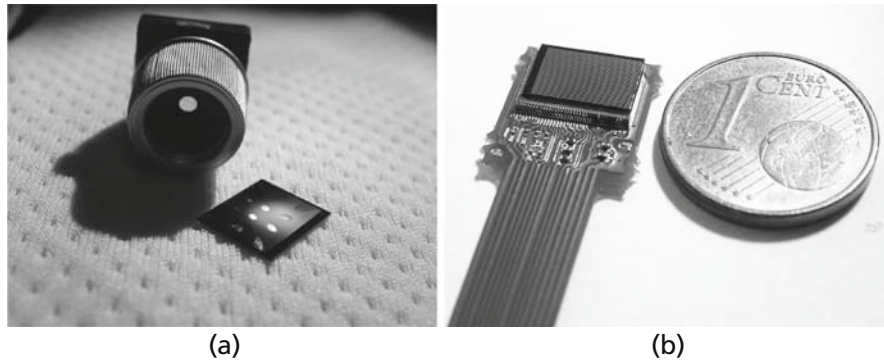


**Fig. 10.7** (a) Size comparison between commercial VGA camera objective (*left*) and artificial apposition compound eye. (b) Ultra-thin vision sensor formed by an artificial apposition com-

pound eye attached to customized CMOS image sensor on flexible carrier

**Table 10.1** Selected parameters of the artificial compound eye prototype from Fig. 10.7b

Parameter/feature	Value
Number of channels	$144 \times 96$
Thickness	$300 \mu\text{m}$
Field of view	$85^\circ \times 51^\circ$
$F/\#$	4
Microlens diameter	$50 \mu\text{m}$
Pixel size	$3 \mu\text{m}$
Size of sensor head	$10 \text{ mm} \times 10 \text{ mm} \times 1.2 \text{ mm}$

cessing capabilities. The sensor size and costs are other important side conditions.

After fabrication, the artificial apposition compound eye objective (shown in Fig. 10.7a) is actively aligned with respect to the image sensor array and finally attached to its surface using transparent glue. The accuracy of the lateral alignment is in the range of  $1\text{--}2 \mu\text{m}$ .

In order to measure and control the quality of fabrication and assembly steps, images of specific test objects are analyzed with respect to resolution, distortion, sensitivity, and brightness homogeneity. Static properties like sampling angle and acceptance angle as well as their variance over several channels are measured. Shading effects and fixed pattern noise are calibrated. For example, a radial star pattern and bar targets of different periods (Fig. 10.8) are well suited to determine the optical resolution limit of such an imaging system.

A critical issue to the performance of artificial apposition compound eyes is the suppression of optical cross-talk. Cross-talk is prevented by using either opaque walls between adjacent channels or by block-

ing unwanted light in horizontal layers of baffle arrays which are placed in different axial depths with decreasing size of apertures toward the image plane (scheme in Fig. 10.9). The first method is also found in nature but it is technologically rather challenging. The second method has the advantage that the necessary thin baffle structures may be easily fabricated by photolithography. For the visualization of cross-talk, the radial star pattern was imaged off-axis by a system with and without baffle layers (Fig. 10.9 right part) under the same conditions. For the artificial apposition compound eye without baffles, a ghost image of the part of the star which is outside the objective's field of view appears on the right side of the image in Fig. 10.9. For the artificial apposition compound eye with additional baffle layers, light from outside the field of view is blocked. Hence, ghost images are suppressed, only the original part of the pattern is imaged, and contrast is preserved. The suppression of optical cross-talk is crucial for multi-aperture imaging sensors if they shall be used for imaging of arbitrary scenes with large field of view.

When using a regular microlens array<sup>10</sup> for imaging a large field of view, large angles of incidence lead to blurring effects within channels that lie outside the center of the array (the blur grows with angle of incidence). However, in each channel a sharp focus is needed for only a narrow angular region independent of the absolute angle of incidence. Thus, the proper-

<sup>10</sup> Here, regular means that all lenslets are exactly the same.



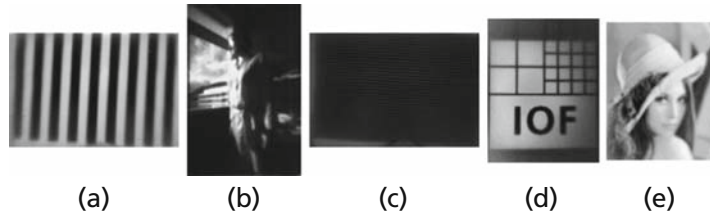


**Fig. 10.8** Test images as captured by the artificial apposition compound eye sensor. (a) Low-frequency bar target. (b) Scientist viewing out of the lab window. (c) High-frequency bar target with 36 LP/field of view. (d) The logo of the Fraunhofer Institute

IOF Jena. (e) A picture of “Image processing Lena.” The original size of all images is  $144 \times 96$  pixels covering a field of view of  $85^\circ \times 51^\circ$ .

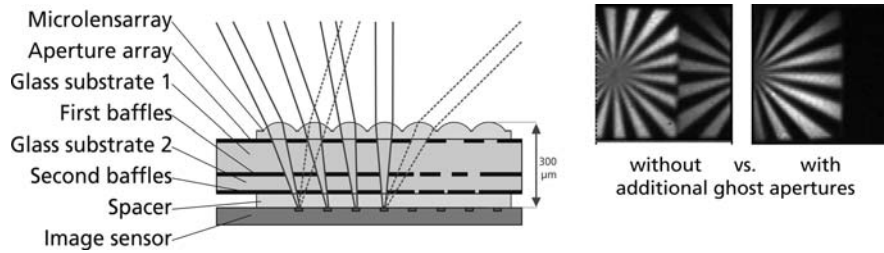


**Fig. 10.9** Schematic section of an artificial apposition compound eye objective with additional baffle aperture arrays for cross-talk suppression. *Solid lines* show useful signal, *dashed lines* show cross-talk. *Right side*: Images of a radial star pattern

which has been moved out of the field of view. *Left image*: Original and ghost image of both halves of the star are clearly visible due to cross-talk. *Right image*: After the introduction of additional baffle arrays the ghost image is suppressed

ties of each microlens in the array can be tuned so that it focuses almost perfectly for its individual angle of incidence. The properties of the individual microlens become a function of the position within the array which is termed “chirped” microlens array [8,48]. The net effect is demonstrated in Fig. 10.10 by comparing between the images of different test patterns captured through a regular and a chirped microlens array (denoted by rMLA and cMLA, respectively) – the resolution is constant for all angles of incidence. It can be clearly observed that the resolution in the center of the field of view is independent of using regular or chirped lens arrays. However, with increasing viewing angle the resolution is decreased in case of the regular microlens array while the resolution remains constant when using the chirped microlens array.

Please note that the proposed tuning of the individual microlenses is an action which is required for a planar compound eye with a large field of view. Nature automatically achieves constant resolution by using lenses on a spherical base structure – so that the lens normal is always parallel to the angle of incidence.

#### 10.4.1.2 Increased Sensitivity with Artificial Neural Superposition

So far, we dealt with crucial issues like the suppression of cross-talk and how to achieve a constant resolution throughout a large field of view. But what about the major drawback of natural apposition compound eyes: Are artificial apposition compound eyes also prone to low sensitivity? Unfortunately, yes. From nature we already know one way to tackle this problem in the context of apposition compound eyes – the neural superposition type.

Adopting the neural superposition type of apposition compound eye is comparatively simple. Instead of a single pixel in the individual channel of the artificial compound eye, a square array of  $n \times n$  pixels is used in each channel of the artificial apposition compound eye. A schematic section of this setup with  $n = 3$  is shown in Fig. 10.11a.

The pitch difference  $\Delta p$  between microlens array and the center of the pixel groups is now defined as

$$\Delta p = p_L - p_K, \quad (10.4)$$

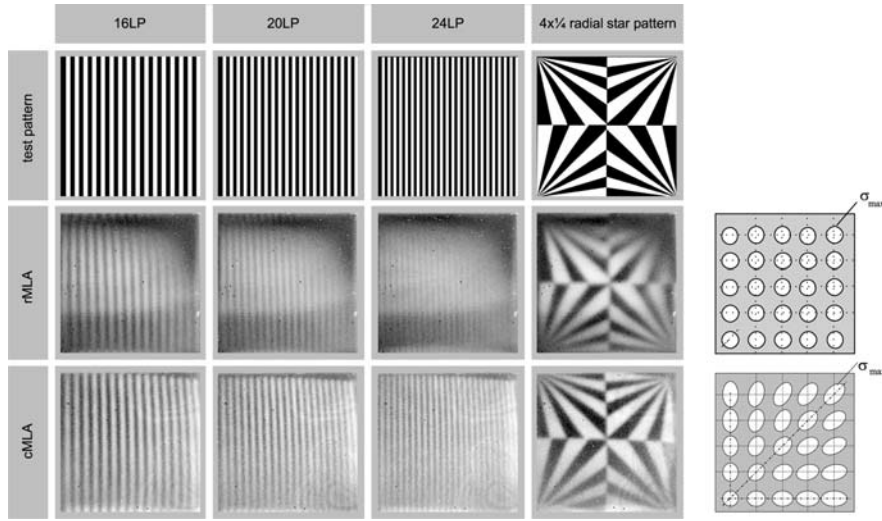


**Fig. 10.10** Bar targets of different spatial frequency and captured images using a chirped microlens array for channel-wise blurring correction under oblique incidence and a regular lens array for comparison. Additionally, a  $4 \times 1/4$  radial star test pattern demonstrates the obtainable resolution in the four image

corners as a function of the angle of incidence. Only one quadrant of the entire symmetrical field of view is shown, so that  $0^\circ$  viewing direction corresponds to the *lower left* corner of each image. The angle of incidence increased up to a maximum of  $\sigma_{\max} = 32^\circ$  in the *upper right* corner of each picture

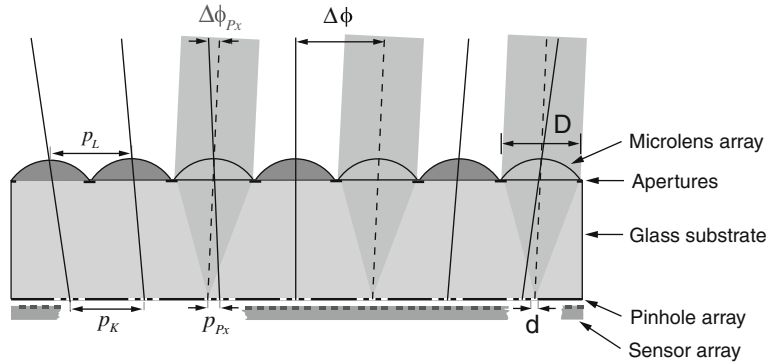


**Fig. 10.11** Schematic layout of the artificial neural superposition eye for increased sensitivity. Each angular segment in object space is imaged in multiple (three shown) pixels of different neighboring channels. In this drawing an image sensor with

small pixel pitch  $p_{Px}$  compared to the size of a single channel  $p_L$  is used. An additional pinhole array is needed on the backside of the artificial compound eye optics to cover unused pixels

and two different sampling angles result. One is the angle between the optical axes of adjacent channels given by Eqs. (10.3, 10.4). The other is defined between adjacent pixels within each channel by

$$\Delta\phi_{Px} = \arctan\left(\frac{p_{Px}}{f}\right). \quad (10.5)$$

By choosing the pitch of the microlens array  $p_L$ , the sampling angle between adjacent channels  $\Delta\phi$  can be set to be a defined fraction of the sampling angle

between pixels  $\Delta\phi_{Px}$ , so that  $m \cdot \Delta\phi = \Delta\phi_{Px}$  holds for integer values of  $m$ . As a result, each object point is imaged on  $n^2$  pixels across  $n^2$  different channels in the 2D microlens array. The recorded signals that belong to a common point in object space are then accumulated to increase the sensitivity. The sensitivity increases proportional to the number of pixels that are involved in the process, e.g.,  $n^2$ , whereas the increase of the signal-to-noise ratio is proportional to the square root of the number of pixels. Due to the redundant sampling this effect is achieved effectively without any

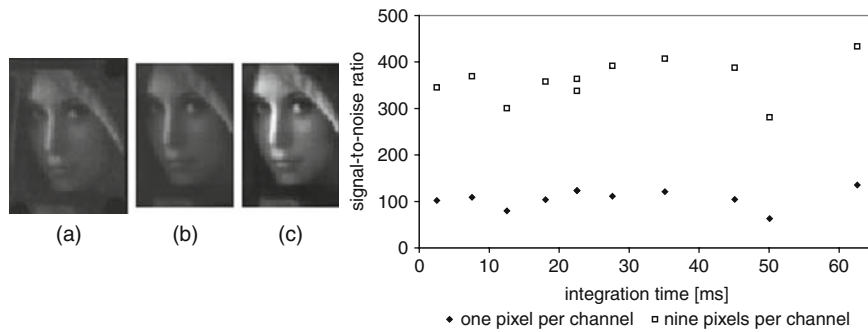


**Fig. 10.12** *Left:* Images of “Lena”: (a) recorded with one pixel per channel, (b) each pixel averaged from nine pixels with common viewing direction (raw image), (c) the same image with normalized gray levels. The image resolution is about  $65 \times 45$  pixels. *Right:* Measured signal-to-noise ratio (SNR) for a system

with (squares) and without (diamonds) artificial neural superposition for different integration times. The signal-to-noise ratio is increased by a factor of three when averaging from nine pixels per field angle

loss of resolution which is demonstrated in Fig. 10.12. However, due to the larger lateral dimensions of the pixel group in each channel and the larger necessary baffle apertures, the suppression of cross-talk in the way that was proposed earlier (Fig. 10.9) becomes less effective in case of a large field of view.

Artificial neural superposition also enables spectral-sensitive imaging using coding of redundant sampled pixels by different spectral filters. Such a scheme is not known of any natural compound eye but it has been used for color imaging with artificial apposition compound eyes [3].

#### 10.4.2 Artificial Superposition Compound Eyes

With a thickness of about 0.3 mm artificial apposition compound eye objectives offer the highest degree of miniaturization for imaging optics, although they require comparatively large lateral dimensions of the image sensor when aiming for a reasonable image resolution<sup>11</sup> because each channel contributes to only one image pixel. For a large number of image pixels, the same large number of channels is needed so that, multiplied by the size of a single channel, a large sensor size results. As an example, for 1000 pixels in one dimension of the image with a channel diameter of 50  $\mu\text{m}$

one would need an image sensor with 50 mm length along one edge. For most applications this would cause unacceptably high costs. This is one of the main reasons why the image resolution of planar artificial apposition compound eyes is restricted to a maximum of about  $200 \times 200$  pixels when using a reasonable size of the image sensor. A way around this stalemate is offered by the Gabor superlens which on the other hand is inspired by the superposition compound eye. Here, a real image is optically formed and can be recorded by a standard image sensor just like it would be the case with a classical single aperture objective. As a result the image resolution can be much higher when using densely packed pixels of small size, allowing small lateral sensor dimensions.

The special type of artificial superposition compound eye demonstrated here consists of three stacked microlens arrays with slightly different pitches which decrease toward the image plane (Fig. 10.13). The first microlens array focuses light from a distant object directly onto a second, so-called field microlens array. A third microlens array re-images the individual intermediate images of each channel onto the final image plane. The pitch difference between the individual arrays causes a deflection of the ray bundles so that the optical axes of the individual channels are tilted with respect to each other and each channel observes a different segment of the field of view<sup>12</sup>. This setup can be interpreted as a cluster of single aperture microcameras

<sup>11</sup> Defined by the total number of pixels in the digital image.

<sup>12</sup> Compared to the artificial apposition compound eye a segment of the individual channel is considerably larger (e.g., by a factor of ten).

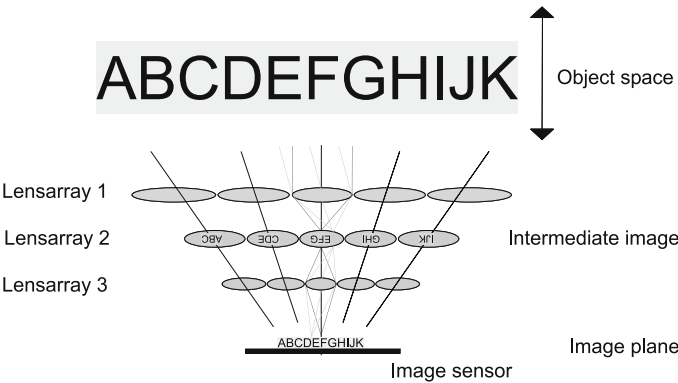


**Fig. 10.13** Working principle of a telescope compound eye imaging system [46]. The arrangement of microlens arrays is similar to that of a Gabor superlens (natural archetype: superposition compound eye). However, internal aperture arrays avoid

which have tilted optical axes to obtain a large overall field of view and is therefore termed “cluster eye” or “CLEY” [47]. The formation of an intermediate image is crucial in order to achieve an array of erect image segments after the re-imaging. Hence, all image segments can be optically stitched together to one single overall image. This feature is different to superposition eyes in insects where each image segment is so large that it overlaps with several neighboring ones, so that light bundles from a large number of channels contribute to the same image point. What is the advantage of image stitching compared to a superposition? The first allows higher resolution whereas the second achieves higher sensitivity.

For lab demonstration, a 2 mm thin prototype of a CLEY has been fabricated and its imaging performance has been evaluated using various test patterns. A detailed list of specifications may be found in Table 10.2. Figure 10.14 shows the images of a page from a textbook, a picture of “Lena,” and the institute logo captured at about 20 cm distance. They demonstrate that a perfect image stitching could not be obtained

superposition in favor for the direct stitching of image segments. Please note that the individual intermediate images are inverted whereas after the re-imaging an array of erect image segments is formed

with this first prototype. Though the image segments are of roughly rectangular shape, they connect or overlap only to some degree (Fig. 10.14a). This causes a considerable intensity modulation even for a homogeneous white object. Nevertheless, the high image contrast and the readability of the text in Fig. 10.14a are promising.

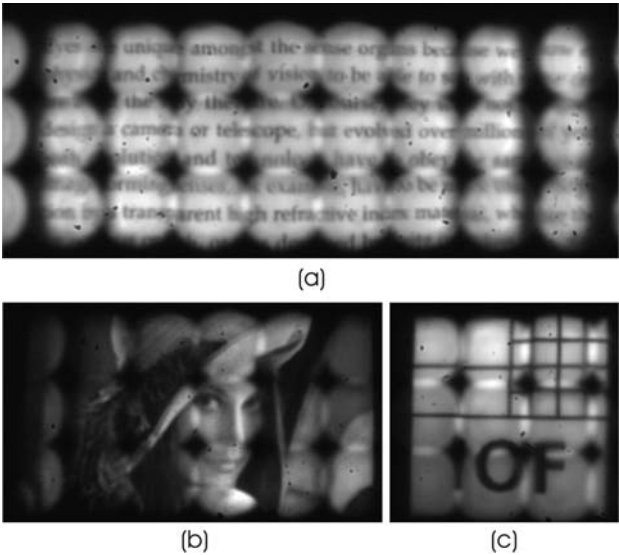


**Table 10.2** List of selected parameters of the prototype of a cluster eye [7].

Parameter/feature	Value
Number of channels	$21 \times 3$
Thickness	2 mm
Total field of view	$70^\circ \times 10^\circ$
Total image size	4.5 mm $\times$ 0.5 mm
Channel FOV	$4.1^\circ \times 4.1^\circ$
Size of image segments	$192 \mu\text{m}^2$

**Fig. 10.14** Experimental demonstration of the imaging capabilities of the cluster eye. (a) Image of a text section of M. F. Land’s book “Animal Eyes,” Sect. 10.3: “What makes a good eye” [31] with size  $10 \times 3.7 \text{ cm}^2$  at a distance of about 20 cm. (b) Image of a picture of “Lena,” and (c) image of the institute logo captured through  $6 \times 3$  channels of the CLEY. Sharp edges and small resolved image features demonstrate the promising imaging capabilities of the cluster eye

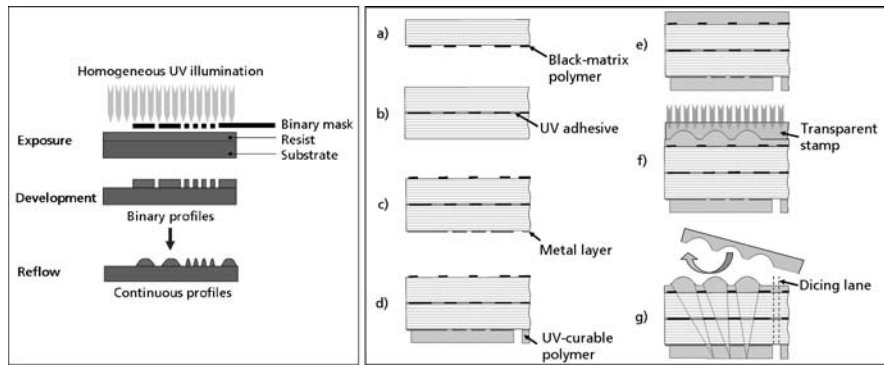


**Fig. 10.15** *Left: Fabrication of a master tool.* A thin resist layer is binary structured by UV exposure through a mask and subsequent reflow creates a smooth surface relief, e.g., spherical microlenses. A negative copy of this master structure acts as replication stamp. *Right: Process flow of the fabrication of an artificial apposition compound eye.* (a) Spin on black-matrix polymer, exposure through mask, development gives an absorbing baffle array layer. (b) Stacking of glass wafers, no precise alignment needed. (c) On the front side the same steps like in (a) are performed, now including alignment. Aligned with respect

to the center baffle array, a thin metal layer is structured, forming a metal baffle array with aperture diameters down to a few microns. (d) Molding of a polymer spacer on the backside. (e) Spin coating of a thin layer of UV-curable polymer on the front. (f) The replication stamp is brought in contact with the polymer resin and UV light is applied through the transparent stamp in order to cure the polymer material. (g) After curing, the stamp is released and the individual objectives are diced by a wafer saw. This technology is carried out in a mask aligner for producing optical microstructures on wafer scale

It is demonstrated that one overall image is generated by the transfer of the different image segments through separated channels with a strong demagnification. The parallel transfer of different parts of an overall field of view (different information) by separated optical channels allows the CLEY to have an overall information capacity which is equal to the sum of the individual channel's capacities. Consequently, the cluster eye has the potential of much higher information capacity (or in other words, a larger number of image pixels) than the demonstrated artificial apposition compound eye. On the other hand the complexity of the CLEY is much higher compared to the artificial apposition compound eye, and it is therefore several times thicker (2 mm instead of 0.3 mm for the apposition type). Additionally, stitching errors might be unavoidable because in case of a cluster eye the tolerances of microlens array fabrication and assembly are very tight (in the order of a few microns) and there are no compensation possibilities without reducing either contrast of the image or degrading the image segment stitching.

### 10.4.3 Fabrication of Artificial Compound Eye Optics

Established processes and equipment of microtechnology are the key enabler for the fabrication of microop-

tical artificial compound eyes. This typically involves coating steps on planar substrates, micropattern generation, and processes to modify and/or transfer the microstructures. A sequence of these process steps requires precise lateral as well as axial alignment (which correspond to a proper centering and focusing of each channel). Here, photolithography is the key implement to achieve the required precision in the micron or even sub-micron range. As a result, millions of features with sub-micron lateral precision are generated in parallel on a planar circular carrier substrate which is referred to as "wafer."<sup>13</sup>

One major task is the fabrication of a master of the actual microstructure like a microlens array (Fig. 10.15 left). This is carried out using a well-established lithography and reflow method [37]. A photoresist material is locally exposed to UV light through a binary mask<sup>14</sup>. After post-processing, binary structures (e.g., array of cylindrical pillars of homogeneous height) remain. These are reflowed so that very smooth and

<sup>13</sup> A process chain which is carried out for many components in parallel on these circular carrier substrates with a diameter of up to 300 mm is called a "wafer scale" process.

<sup>14</sup> Binary photomasks have apertures allowing the UV light to locally expose the underlying polymer and opaque regions that block UV light.

precise spherical surface profiles are created due to the surface tension. Finally, a transparent replication stamp is formed as a negative copy of the wafer which carries the master structures.

A simplified flow of an example fabrication process of an artificial compound eye objective is shown on the right side in Fig. 10.15. Thin glass wafers are the substrate material of choice due to their high optical transparency and mechanical stability at low thickness (usually less than 0.2 mm). Two glass wafers are bonded/glued together to form the baffle setup of an apposition compound eye as shown in Fig. 10.9. Subsequently, baffle arrays of different sizes are patterned by photolithography in thin layers of light-absorbing (black-matrix) polymer. The transparent stamp with the negative microstructure is pressed into the polymer using a modified contact mask aligner (see Fig. 10.16) [4,18]. The polymer hardens by applying UV light through the stamp and its microstructure relief is fixed even after removing the stamp. Here the axial precision of about  $\pm 5\mu\text{m}$  is limited by the bowing of the substrate, tool, and reference backplane as well as axial (z-axis) positioning and wedge errors, whereas the lateral precision of  $\pm 1\mu\text{m}$  is similar to that of photolithography.

The UV cross-linking of spacer, aperture, and lens polymers provides the chemical and temperature stability which is necessary to combine all the patterning steps in arbitrary order and to ensure the compatibility to subsequent processes like bonding/soldering or

dicing. In principle, our approach allows the assembly of apposition compound eye objectives with Si-based CMOS or CCD imager sensors on a wafer scale and the subsequent separation using a dicing saw. Alternatively, separated optical chips can be aligned and bonded to electrically connected image sensors.

#### 10.4.4 Future Challenges

One of the main issues for the future would be to achieve a closer interaction between the compound eye optics and the optoelectronic components. For example, for the application to flying/moving vehicles we aim for the symbiosis of artificial apposition compound eyes with smart image sensors that work highly parallel with pixel-wise embedded optical flow detection (see Chap. 3 for details). For such application, size and weight advantages of compound eye optics would perfectly complement with fast-processing abilities and high dynamic range of such sensors. Considering the lateral dimensions, optical flow detection chips need a large pixel size for implementing the processing circuits within the periphery of the photodiodes, which is exactly provided by an artificial apposition compound eye due to the large lens diameter compared to the size of the single photodiode within its footprint.

Optical sensors that work in very close object distance or at high speed (e.g., optical mice navigation sensors) might benefit from the integration of solid-state illumination (e.g., LEDs or organic LEDs) on-chip with the image sensor and compound eye optics. Optical channels for distributing the illumination light onto the object might be situated periodically next to the imaging channels in order to create an overall integrated system.

Great potential lies in the realization of compound eyes on a curved basis as this is not only an evolutionary but also a physical optimum for tiny optical systems. A spherical shell offers the largest surface area with smallest possible volume, so that highest miniaturization can be achieved with the largest possible number of ommatidia (i.e., best possible resolution). Besides, each ommatidium images close to perpendicular incidence which allows very simple spherical lens profiles and a large field of view results by

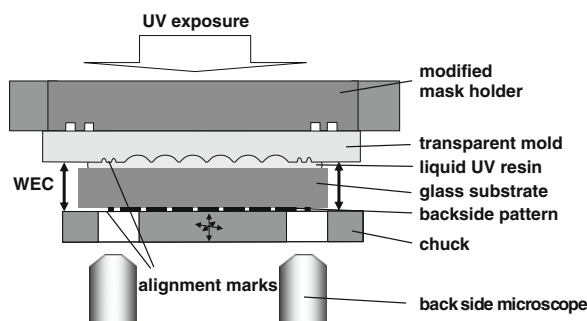


**Fig. 10.16** Molding of polymer-on-glass microlens arrays on wafer scale using a modified mask aligner. The aligner reference backplane (chuck) fixes the substrate with the mold and eliminates the tilt between them (wedge error compensation, WEC). Lateral alignment is carried out by x,y stages and microscopes, the z-motion controls the polymer thickness (axial alignment). After UV exposure and separation, a polymer replication of the lens array remains on the glass wafer



default. However, most challenges here are of technological nature. Up to date, a few examples of fabricating microlens arrays on non-planar substrates have been demonstrated [32,38]. However, the major problem of recording the image from a curved image plane remains. Some proposed ways like thinning of standard planar image sensors or using a grid of thin photodiodes on a flexible sheet and subsequently bowing the thin sensor array [27] seem to be sporadic attempts to come around this problem, but are usually applicable only along one dimension. Organic photodiodes seem to be a promising solution for non-planar detector arrays if they reach a high efficiency with small pixel sizes and a moderate lifetime.

Artificial apposition compound eyes demonstrated the highest miniaturization known to imaging systems so far. On the other hand, the comparatively low resolution limits their application to machine vision and optical navigation sensors. In the future, it has to be further increased for most applications in the fields of medical imaging, security, and consumer products. Ongoing efforts also deal with exploring the possibilities and technological realization of more sophisticated versions of compound eyes such as the Gabor superlens (Sect. 10.4) or the cluster eye. Preliminary simulation results promise good image resolution of  $350 \times 350$  pixels in combination with a high sensitivity ( $F/\# = 1.5$ ) for a modified Gabor superlens system of about 2 mm thickness. On the other hand, we aim for the optimization of image stitching properties for the cluster eye (which was described in Sect. 10.4.2) to achieve about  $640 \times 480$  pixels (VGA) resolution. Such a system would be able to compete with small classical single-aperture objectives.

Although several critical issues for the realization and application of artificial compound eyes seem to be solved by the different approaches we presented here, there is much more work to be done. Microoptical imaging sensors are still in their advent so that it will take another 5 years from now until the first products will be on the market. However, the application of artificial compound eyes in flying micro-robots (e.g., for the purpose of search and rescue or as a toy) may play a leading role for the ongoing development of these sensors.

**Acknowledgments** We would like to thank Sylke Kleinle, Andre Matthes, Antje Oelschläger, and Simone Thau from the Fraunhofer Institute for Applied Optics and Precision Engineer-

ing (IOF), Jena, for their contributions to the fabrication of the various types of artificial apposition compound eye objectives using microoptics technology. Special thanks is dedicated to Reinhard Völkel from SUSS MicroOptics SA (Neuchâtel, Switzerland) for his inspiring previous work and helpful discussions about bio-inspired imaging. The experience of Martin Eisner (also SUSS MicroOptics) in aligned stacking of microlens array wafers finally led to the realization of the cluster eye. We are furthermore very thankful for the help we got from our colleagues from the Institute of Microtechnology (IMT) of the University of Neuchâtel, Switzerland, especially Toralf Scharf who took very important steps in the fabrication of the lens- and aperture arrays of the cluster eye. The presented work was partly funded by the German Federal Ministry of Education and Research (BMBF) within the project "Extremely compact imaging systems for automotive applications" (FKZ: 13N8796).

## References

1. Barlow, H.B.: The size of ommatidia in apposition eyes. *Journal of Experimental Biology* **29**, 667–674 (1952)
2. Borrelli, N.F., Bellman, R.H., Durbin, J.A., Lama, W.: Imaging and radiometric properties of microlens arrays. *Applied Optics* **30**(25), 3633–3642 (1991)
3. Brückner, A., Duparré, J., Dannberg, P., Bräuer, A., Tünnermann, A.: Artificial neural superposition eye. *Optics Express* **15**(19), 11,922–11,933 (2007)
4. Dannberg, P., Mann, G., Wagner, L., Bräuer, A.: Polymer UV-molding for micro-optical systems and O/E- integration. In: S.H. Lee, E.G. Johnson (eds.) *Proc. of Micromachining for Micro-Optics*, vol. SPIE **4179**, 137–145 (2000)
5. Duparré, J., Dannberg, P., Schreiber, P., Bräuer, A., Tünnermann, A.: Artificial apposition compound eye fabricated by micro-optics technology. *Applied Optics* **43**(22), 4303–4310 (2004)
6. Duparré, J., Dannberg, P., Schreiber, P., Bräuer, A., Tünnermann, A.: Thin compound eye camera. *Applied Optics* **44**(15), 2949–2956 (2005)
7. Duparré, J., Schreiber, P., Matthes, A., Pshenay-Severin, E., Bräuer, A., Tünnermann, A., Völkel, R., Eisner, M., Scharf, T.: Microoptical telescope compound eye. *Optics Express* **13**(3), 889–903 (2005)
8. Duparré, J., Wippermann, F., Dannberg, P., Reimann, A.: Chirped arrays of refractive ellipsoidal microlenses for aberration correction under oblique incidence. *Optics Express* **13**(26), 10,539–10,551 (2005)
9. Franceschini, N., Pichon, J.M., Blanes, C.: From insect vision to robot vision. *Philosophical Transactions: Biological Sciences*. The Royal Society is the publisher, see: <http://www.jstor.org/pss/57060>. Series B **337**, 283–294 (1992)
10. Gabor, D.: Improvements in or relating to optical systems composed of lenticules. Pat. UK 541,753 (1940)
11. Goetz, K.G.: Die optischen Uebertragungseigenschaften der Komplexaugen von *Drosophila*. *Kybernetik* **2**, 215–221 (1965)
12. Hamanaka, K., Koshi, H.: An artificial compound eye using a microlens array and its application to scale-invariant processing. *Optical Review* **3**(4), 264–268 (1996)

13. Hardie, R.: Functional organization of the fly retina. *Progress in Sensory Physiology* **5**, 1–79 (1985)
14. Hembd-Sölner, C., Stevens, R.F., Hutley, M.C.: Imaging properties of the Gabor superlens. *Journal of Optics A: Pure and Applied Optics* **1**, 94–102 (1999)
15. Horridge, G.A.: The compound eye of insects. *Scientific American* **237**, 108–120 (1977)
16. Horridge, G.A.: The separation of visual axes in apposition compound eyes. *Philosophical transactions of the Royal Society of London. Series B* **285**, 1–59 (1978)
17. Hoshino, K., Mura, F., Shimoyama, I.: A One-chip Scanning Retina with an Integrated Micromechanical Scanning Actuator. *Journal of Microelectromechanical System* **10**(4), 492–497 (2001)
18. Houbertz, R., Domann, G., Cronauer, C., Schmitt, A., Martin, H., Park, J.U., Fröhlich, L., Buestrich, R., Popall, M., Streppel, U., Dannberg, P., Wächter, C., Bräuer, A.: Inorganic-Organic Hybrid Materials for Application in Optical Devices. *Thin Solid Films* **442**, 194–200 (2003)
19. Hugle, W.B., Daendliker, R., Herzig, H.P.: Lens array photolithography. *Pat. US* 8,114,732 (1993)
20. Hutley, M.C.: Integral photography, superlenses and the moiré magnifier. In: M.C. Hutley (ed.) *Digest of Top. Meet. on Microlens Arrays at NPL, Teddington*, vol. EOS **2**, pp. 72–75 (1993)
21. Jeong, K., Kim, J., Lee, L.P.: Polymeric synthesis of biomimetic artificial compound eyes. *Proceedings of the 13th International Conference on Solid-State Sensors, Actuators and Microsystems (Transducers 05)*, pp. 1110–1114 (2005)
22. Kamal, H., Völkel, R., Alda, J.: Properties of moiré magnifiers. *Optical Engineering* **37**(11), 3007–3014 (1998)
23. Kawazu, M., Ogura, Y.: Application of gradient-index fiber arrays to copying machines. *Applied Optics* **19**(7), 1105–1112 (1980)
24. Kirschfeld, K.: The resolution of lens and compound eyes. *Neural Principles in Vision* pp. 354–370 (1976)
25. Kirschfeld, K., Franceschini, N.: Optical characteristics of ommatidia in the complex eye of musca. *Kybernetik* **5**, 47–52 (1968)
26. Kitamura, Y., Shogenji, R., Yamada, K., Miyatake, S., Miyamoto, M., Morimoto, T., Masaki, Y., Kondou, N., Miyazaki, D., Tanida, J., Ichioka, Y.: Reconstruction of a high-resolution image on a compound-eye image-capturing system. *Applied Optics* **43**(8), 1719–1727 (2004)
27. Ko, H.C., Stoykovich, M.P., Song, J., Malyarchuk, V., Choi, W.M., Yu, C.J.: A hemispherical electronic eye camera based on compressible silicon optoelectronics. *Nature* **454**, 748–753 (2008)
28. Land, M.F.: Compound eyes: Old and new optical mechanisms. *Nature* **287**, 681–686 (1980)
29. Land, M.F.: Variations in Structure and Design of Compound Eyes. In: D. Stavenga, R.C. Hardie (eds.) *Facets of Vision*, Chap. 5, pp. 90–111. Springer (1989)
30. Land, M.F., Burton, F., Meyer-Rochow, V.: The Optical Geometry of Euphausiid Eyes. *Journal of Comparative Physiology A* **130**(1), 49–62 (1979)
31. Land, M.F., Nilsson, D.E.: *Animal Eyes*. Oxford Animal Biology Series. Oxford University Press, Oxford (2002)
32. Lee, L.P., Szema, R.: Inspirations from biological optics for advanced photonic systems. *Science* **310**(5751), 1148–1150 (2005)
33. Lohmann, A.W.: Scaling laws for lens systems. *Applied Optics* **28**(23), 4996–4998 (1989)
34. McIntyre, P., Caveney, S.: Graded index optics are matched to optical geometry in the superposition eyes of scarab beetles. *Philosophical Transactions of the Royal Society of London. Series B* **311**, 237–269 (1985)
35. Nakayama, K.: Biological image motion processing: a review. *Vision Research* **25**(5), 625–660 (1985)
36. Ogata, S., Ishida, J., Sasano, T.: Optical sensor array in an artificial compound eye. *Optical Engineering* **33**(11), 3649–3655 (1994)
37. Popovich, Z.D., Sprague, R.A., Conell, G.A.N.: Technique for monolithic fabrication of microlens arrays. *Applied Optics* **27**(7), 1281–1284 (1988)
38. Radtke, D., Duparré, J., Zeitner, U., Tünnermann, A.: Laser lithographic fabrication and characterization of a spherical artificial compound eye. *Optics Express* **15**, 3067–3077 (2007)
39. Sanders, J.S. (ed.): *Selected Papers on Natural and Artificial Compound Eye Sensors*, 122 edn. SPIE Milestone Series. SPIE Optical Engineering Press, Bellingham (1996)
40. Sanders, J.S., Halford, C.E.: Design and analysis of apposition compound eye optical sensors. *Optical Engineering* **34**(1), 222–235 (1995)
41. Smith, W.J.: *Modern Optical Engineering: The Design of Optical Systems*, 2 edn. McGraw-Hill, New York (1990)
42. Snyder, A.W.: *Physics of Vision in Compound Eyes*. Handbook of sensory physiology, pp. 225–313. Springer (1977)
43. Snyder, A.W., Stavenga, D.G., Laughlin, S.B.: Spatial Information Capacity of Compound Eyes. *Journal of Comparative Physiology A* **116**, 183–207 (1977)
44. Stevens, R.F.: Optical inspection of periodic structures using lens arrays and moiré magnification. *Imaging Science Journal* **47**, 173–179 (1999)
45. Thorson, J.: Small-signal analysis of a visual reflex in the locust. *Kybernetik* **3**(2), 41–66 (1966)
46. Völkel, R., Eisner, M., Weible, K.J.: Miniaturized imaging systems. *Microelectronic Engineering* **67–68**, 461–472 (2003)
47. Völkel, R., Wallstab, S.: Flachbauendes Bilderfassungssystem. *Pat. DE* 199 17 890A1 (1999)
48. Wippermann, F., Duparré, J., Schreiber, P., Dannberg, P.: Design and fabrication of a chirped array of refractive ellipsoidal micro-lenses for an apposition eye camera objective. In: L. Mazuray, R. Wartmann (eds.) *Proceedings of Optical Design and Engineering II*, vol. 5962, pp. 59,622C–1–59,622C–11 (2005)
49. Yamada, K., Tanida, J., Yu, W., Miyatake, S., Ishida, K., Miyazaki, D., Ichioka, Y.: Fabrication off diffractive microlens array for opto-electronic hybrid information system. *Proceedings of Diffractive Optics' 99*, pp. 52–53. EOS (1999)